LBNL-39251
UC-414

# ERNEST ORLANDO LAWRENCE BERKELEY NATIONAL LABORATORY

# Strong WW Scattering Chiral Lagrangians, Unitarity and Resonances

J.R. Peláez
**Physics Division**

August 1996
To be presented at the
*American Physical Society New Direction for High Energy Physics,*
Snowmass, Colorado,
July 25–Aug. 2, 1996;
and to be published in
the Proceedings

REFERENCE COPY
Does Not
Circulate
Bldg. 50 Library.
Copy 1
LBNL-39251

## DISCLAIMER

This document was prepared as an account of work sponsored by the United States Government. While this document is believed to contain correct information, neither the United States Government nor any agency thereof, nor the Regents of the University of California, nor any of their employees, makes any warranty, express or implied, or assumes any legal responsibility for the accuracy, completeness, or usefulness of any information, apparatus, product, or process disclosed, or represents that its use would not infringe privately owned rights. Reference herein to any specific commercial product, process, or service by its trade name, trademark, manufacturer, or otherwise, does not necessarily constitute or imply its endorsement, recommendation, or favoring by the United States Government or any agency thereof, or the Regents of the University of California. The views and opinions of authors expressed herein do not necessarily state or reflect those of the United States Government or any agency thereof or the Regents of the University of California.

LBL-39251
UC-414

# Strong WW Scattering
# Chiral Lagrangians, Unitarity and Resonances

J.R. Peláez

Physics Division
Ernest Orlando Lawrence Berkeley National Laboratory
University of California
Berkeley, California 94720

August 1996

This work was supported by the Director, Office of Energy Research, Office of High Energy and Nuclear Physics, Division of High Energy Physics, of the U.S. Department of Energy under Contract No. DE-AC03-76SF00098.

LBNL-39251

# Strong WW Scattering Chiral Lagrangians, Unitarity and Resonances [1]

J. R. Peláez[2]
*Theoretical Physics Group*
*Ernest Orlando Lawrence Berkeley National Laboratory*
*University of California, Berkeley, California 94720*

ABSTRACT

Chiral lagrangians provide a model independent description of the strongly interacting symmetry breaking sector. In this work it is first reviewed the LHC sensitivity to the chiral parameters (in the hardest case of non-resonant low-energy WW scattering). Later it is shown how to reproduce or predict the resonance spectrum by means of dispersion theory and the inverse amplitude method. We present a parameter space scan that covers many different strong WW scattering scenarios.

Talk presented at the:
1996 DPF/DPB Summer Study on New Directions for High-Energy Physics.
(Snowmass 96).

[1] This work was supported by the Director, Office of Energy Research, Office of High Energy and Nuclear Physics, Division of High Energy Physics of the U.S. Department of Energy under Contract DE-AC03-76SF00098.

[2] Complutense del Amo fellow. On leave of absence from Departamento de Física Teórica. Univ. Complutense. 28040 Madrid, Spain.

# Strong WW Scattering
# Chiral Lagrangians, Unitarity and Resonances *

J. R. Peláez*
*Theoretical Physics Group*
*Ernest Orlando Lawrence Berkeley National Laboratory*
*University of California, Berkeley, California 94720*

## ABSTRACT

Chiral lagrangians provide a model independent description of the strongly interacting symmetry breaking sector. In this work it is first reviewed the LHC sensitivity to the chiral parameters (in the hardest case of non-resonant low-energy WW scattering). Later it is shown how to reproduce or predict the resonance spectrum by means of dispersion theory and the inverse amplitude method. We present a parameter space scan that covers many different strong WW scattering scenarios.

## I CHIRAL LAGRANGIANS

### A Introduction

In the Standard Model (SM) there is an spontaneous symmetry breaking of the gauge $SU(2)_L \times U(1)_Y$ group down to $U(1)_{EM}$. The underlying theory that produces this mechanism is unknown to a large extent. Basically, what we know is the following:

- There is a system with a global symmetry breaking from a group $G$ down to another one $H$ producing three Goldstone bosons (GB).
- The scale of this new interactions is $v \simeq 250$GeV.
- The electroweak $\rho$ parameter is very close to one.

This last requirement is most naturally satisfied if the electroweak Symmetry Breaking Sector (EWSBS) respects the so called custodial symmetry $SU(2)_{L+R}$ [1]. Demanding just three GB, we are lead to $G = SU(2)_L \times SU(2)_R$ and $H = SU(2)_{L+R}$ [2, 3].

That is the very same breaking pattern of chiral symmetry in QCD with two massless quarks. It is well known that a rescaled version of QCD is not valid as an EWSBS. However, we still can borrow the formalism of chiral lagrangians [4], known as Chiral Perturbation Theory (ChPT), which works remarkably well for pion physics [5].

Our case is different to QCD since, among other things, the GB disappear in the Higgs mechanism. They become the longitudinal components of the gauge bosons. Hence, if we want to probe an strong EWSBS, we actually have to look at interactions of longitudinal gauge bosons. (We will denote both $W$ and $Z$ by $V$). Indeed if the EWSBS is strongly interacting, we expect an enhancement in $V_L$ production. That is why we are interested in $V_L V_L$ scattering.

### B The Low energy Theorems

The chiral lagrangian is built as a (covariant) derivative expansion out of GB fields. Only those operators respecting the above symmetry pattern and Lorentz invariance are allowed (we are also neglecting CP violation). Thus, there is only one possible term with two derivatives:

$$\mathcal{L}^{(2)} = \frac{v^2}{4} \mathrm{tr} D_\mu U D^\mu U^\dagger \tag{1}$$

where the GB fields $\pi^i$ are collected in the $SU(2)$ matrix $U = \exp(i\pi^i\sigma^i/v)$ and $D_\mu$ is the usual covariant derivative.

The above lagrangian is able to describe the very low energy behavior of the EWSBS. However it will be useful when *only* the GB and the gauge fields are relevant at low energies. That is the case of the strong EWSBS since the other particles affecting $VV$ scattering (like resonances) are expected at the TeV scale.

It is important to remark that the lagrangian in Eq.1 only depends on the symmetry structure and the scale. Its predictions for $V_L V_L$ scattering are therefore universal. The two derivatives become external momenta and thus this term yields $\mathcal{O}(p^2)$ contributions, which are called the Low Energy Theorems (LET) [2].

### C The $\mathcal{O}(p^4)$ lagrangian.

The lagrangian in Eq.1 is that of a non-linear $\sigma$ model. Thus, in a strict sense it is non-renormalizable. However, all the divergencies appearing at one loop are $\mathcal{O}(p^4)$ and can be absorbed in the parameters of the $\mathcal{L}^{(4)}$ lagrangian. If we were to consider two loops with $\mathcal{L}^{(2)}$ we would need the $\mathcal{L}^{(6)}$ lagrangian and so on. The relevant point is that up to a given order in the external momenta the calculations can be renormalized and are finite.

There are many terms in the $\mathcal{L}^{(4)}$ lagrangian [6], although for $VV$ scattering at $\mathcal{O}(p^4)$ it is enough to consider:

$$\begin{aligned}\mathcal{L}^{(4)} &= L_1 \left(\mathrm{tr} D_\mu U D^\mu U^\dagger\right)^2 + L_2 \left(\mathrm{tr} D_\mu U D^\nu U^\dagger\right)^2 \\ &+ i\mathrm{tr}\left[(L_{9L} W^{\mu\nu} + L_{9R} B^{\mu\nu}) D_\mu U D_\nu U^\dagger\right] \\ &+ L_{10} \mathrm{tr} U^\dagger B^{\mu\nu} U W_{\mu\nu}\end{aligned} \tag{2}$$

where $W^{\mu\nu}$ and $B^{\mu\nu}$ are the strength tensors of the gauge fields. Only the values of the $L_i$ parameters depend on the underlying theory.

*This work was supported by the Director, Office of Energy Research, Office of High Energy and Nuclear Physics, Division of High Energy Physics of the U.S. Department of Energy under Contract DE-AC03-76SF00098.

[1] Complutense del Amo fellow. On leave of absence from Departamento de Física Teórica. Univ. Complutense. 28040 Madrid, Spain.

For our purposes, we are only interested in $L_2$ and $L_1$, which are the ones that enter the $VV$ fusion calculations. The others are related to anomalous couplings. Their values can be estimated for the minimal SM (MSM) with a heavy Higgs [7] as well as for QCD-like models (using the ChPT parameters [8]). In Table I we give some reference values. Notice that in the literature it is also frequent to extract a $16\pi^2$ factor so that the $L_i$ are of order unity.

Table I: Chiral Parameters for different reference models.

| | $L_1$ | $L_2$ |
|---|---|---|
| MSM ($M_H \sim 1$ TeV) | 0.007 | -0.002 |
| QCD-like | -0.001 | 0.001 |

Using the lagrangians in Eqs.1 and 2 we can calculate the $VV$ elastic scattering amplitudes. Indeed they are obtained as a truncated series in $p/4\pi v$, as follows:

$$t(s) \simeq t^{(0)}(s) + t^{(1)}(s) + \mathcal{O}(p^6) \qquad (3)$$

Where $t^{(0)}(s)$ is $\mathcal{O}(p^2)$ and reproduces the LET. It is obtained from $\mathcal{L}^{(2)}$ at tree level. The $t^{(1)}(s)$ contribution is $\mathcal{O}(p^4)$ and comes from the $\mathcal{L}^{(4)}$ at tree level and $\mathcal{L}^{(2)}$ at one loop. If we made one more loop we would get $\mathcal{O}(p^6)$ contributions, and we would need the $\mathcal{L}^{(6)}$ lagrangian, etc...

Note that a naive estimate of the applicability range is $4\pi v \lesssim 3$TeV. However, the existence of resonances will limit the effectiveness of the approach up to $\lesssim 1.5$TeV.

## D Chiral parameters at LHC

The goal of future accelerators is to determine the nature of the EWSBS. As we have seen, chiral lagrangians provide a model independent formalism. We always deal with the same set of operators and only the actual values of the parameters depend on the fundamental theory.

As we have already stressed the most natural channel to look for strong EWSBS interactions is $V_L V_L$ scattering. The most striking experimental feature would be the appearance of resonant states. However, it is not assured that they could be directly seen in the next generation of colliders. Even though they are expected at the TeV scale, they can be higher that the planned energy reach. In that case one is left with a non-resonant behavior, where different models will be hard to distinguish. Then the effective lagrangians become a natural and systematic tool to parametrize and maybe disentangle the experimental results.

Indeed there are already some studies of the capability of LHC to measure the chiral parameters [9]. In Table II are listed the number of events produced with various non vanishing values of $L_2$ or $L_1$. Following reference [9] we have recalculated the results for 100fb$^{-1}$ of integrated luminosity at $\sqrt{14}$TeV. That corresponds to one experiment collecting data at full design luminosity during one year.

The numbers in Table II are those of the cleanest leptonic decays of subprocesses whose final state is either $W^\pm Z$ or $ZZ$:

$$\begin{array}{lll} q\bar{q}' \to W^\pm Z & q\bar{q} \to ZZ & gg \to ZZ \\ W^\pm Z \to W^\pm Z & ZZ \to ZZ & \\ W^\pm \gamma \to W^\pm Z & W^+W^- \to ZZ & \end{array}$$

They have been calculated from the lagrangian in Eqs.1 and 2 at tree level (except gluon fusion, that only occurs at one loop). All possible initial and final helicity combinations have been considered. We use the effective W approximation, but *not* the Equivalence Theorem. By the cleanest leptonic modes we mean the $W$'s and the $Z$'s decaying to $\nu_e e, \nu_\mu \mu$ and $e^- e^+, \mu^- \mu^+$, respectively. The corresponding branching ratios are BR(WZ)=0.013 and BR(ZZ)=0.0044. We have also imposed a set of minimal cuts: $M_{VV}^{\max} = 1.5$TeV, $P_{T\,min}^Z = 300$GeV, $y_{max}^V = 2$. Further details of the calculation can be found in [9].

Table II: Number of events and statistical significances for different values of $L_2$ and $L_1$ at LHC.

| | $10^{-2}$ | $-10^{-2}$ | $5\times10^{-3}$ | $-5\times10^{-3}$ |
|---|---|---|---|---|
| | $L_1$ | | | |
| $W^\pm Z^0 \to W^\pm Z^0$ | 22 | 58 | 23 | 41 |
| total $W^\pm Z^0$ | 104 | 139 | 105 | 122 |
| $r_5\|_{W^\pm Z^0}$ | 0.7 | 2.6 | 0.6 | 1.0 |
| $r_5\|_{W^\pm Z^0\ tagging}$ | 1.0 | 4.2 | 0.9 | 1.7 |
| $W^+W^- \to Z^0Z^0$ | 21 | 7 | 13 | 6 |
| $Z^0Z^0 \to Z^0Z^0$ | 6 | 6 | 1 | 1 |
| total $Z^0Z^0$ | 46 | 32 | 33 | 26 |
| $r_5\|_{Z^0Z^0}$ | 3.8 | 0.9 | 1.2 | 0.1 |
| $r_5\|_{Z^0Z^0\ tagging}$ | 6.6 | 1.8 | 2.3 | 0.2 |
| | $L_2$ | | | |
| $W^\pm Z^0 \to W^\pm Z^0$ | 36 | 80 | 27 | 47 |
| total $W^\pm Z^0$ | 118 | 162 | 109 | 129 |
| $r_4\|_{W^\pm Z^0}$ | 0.7 | 4.8 | 0.2 | 1.7 |
| $r_4\|_{W^\pm Z^0\ tagging}$ | 1.0 | 7.5 | 0.3 | 2.7 |
| $W^+W^- \to Z^0Z^0$ | 12 | 7 | 9 | 7 |
| $Z^0Z^0 \to Z^0Z^0$ | 6 | 6 | 1 | 1 |
| total $Z^0Z^0$ | 37 | 32 | 30 | 27 |
| $r_4\|_{Z^0Z^0}$ | 1.9 | 0.9 | 0.5 | $\simeq 0$ |
| $r_4\|_{Z^0Z^0\ tagging}$ | 3.5 | 1.8 | 0.9 | 0.1 |

The statistical significances are defined with respect to the "zero" model (when all the $L_i$ are set to zero). In [9] they are also given with respect to the SM with $M_H \simeq$ 1TeV. Note that the zero model is nothing but the LET predictions or the $M_H \to \infty$ limit of the MSM. The statistical significances are defined as:

$$r_i = \frac{|N(L_i) - N(0)|}{\sqrt{N(0)}} \qquad (4)$$

In Table II we have listed two sensitivities for each process depending on whether there is forward jet tagging available or not. This detector feature is very important to separate those events coming from $VV$ fusion from those coming from quarks. We have given numbers for no jet tagging at all and 100% efficiency tagging, so that the real number will lie somewhere in between.

The analysis is simplified in the sense that only one $L_i$ is different from zero at a time. However, there are issues that could improve the sensitivity that we have not addressed. We have only restricted ourselves to leptonic modes, and we have not studied the $W^+W^-$ or the $W^\pm W^\pm$ final states. The sensitivities only refer to separate channels and a simultaneous fit to all them would be a considerable improve. There is still open the possibility of final state polarization analysis that would enhance the longitudinal modes. Finally we are also confident that more elaborated cuts will also enhance the signal. Therefore, we think that the numbers in Table II can be considered as a conservative estimate of the LHC capabilities.

From Table II we can thus see that the $10^{-2}$ values are at hand at the $3\sigma$ level, both for $L_2$ and $L_1$. Combining the two experiments and one or two years of running even the $5\sigma$ level seems attainable.

It is convenient at this point to look back at Table I and notice that the expected values lie on the range $10^{-2}$ to $10^{-3}$. Therefore, we can easily reach the beginning of the interesting region. Notice also that the two reference models have different signs in their parameters. Fortunately the experimental signature is radically different when changing the sign of the parameters. It seems feasible to differentiate positive from negative signs.

To go down to the level of $L_i = 5 \times 10^{-3}$ its harder, but not impossible. The $3\sigma$ level seems reachable in three or four years in many channels, by combining the two experiments. We have not listed the results for $10^{-3}$ since that level of precision seems extremely hard to access [9].

It is important to remark again that this is a preliminary and conservative result. We can conclude that even in the non-resonant scenario, LHC will be able to test at least *part* of the chiral parameter space in the interesting region. It is also clear that the study of this kind of physics will require the ultimate machine performance.

As we will see in the next section the determination of $L_1$ and $L_2$ will be very helpful to disentangle the nature of an strong EWSBS. Even if the LHC energy reach is not enough to observe resonances directly, their existence can be established by means of dispersion theory.

# II UNITARITY AND RESONANCES

## A Elastic unitarity

Up to now we have not considered possible resonant states. Resonances are one of the most characteristic features of strong interactions. In our case, we expect them to appear at the 1 TeV scale. For instance, the MSM becomes strong when $M_H \simeq 1$TeV. In such case we expect a very broad scalar resonance around 1 TeV. In QCD-like models one expects a vector resonance around 2 TeV.

From now on it will be very convenient to use amplitudes of definite angular momentum $J$. As far as we also have a conserved $SU(2)_{L+R}$ symmetry in the EWSBS, we can also define a weak isospin $I$. In analogy to $\pi\pi$ scattering, we will then have three possible isospin channels $I = 0, 1, 2$. At low energies we are only interested in the lowest $J$, and thus we will concentrate on the $t_{IJ} = t_{00}, t_{11}$ and $t_{20}$ partial waves. Indeed we will present our results in terms of their complex phases, which are know as phase shifts.

Chiral lagrangians by themselves are not able to reproduce resonances. Their amplitudes are obtained as polynomials in the momenta and masses, and therefore they do not even satisfy the elastic unitarity condition:

$$\mathrm{Im} t_{IJ}(s) = \sigma(s)|t_{IJ}(s)|^2 \tag{5}$$

where $\sigma(s)$ is the two body phase-space. Nevertheless, they satisfy it *perturbatively*

$$\mathrm{Im} t^{(1)}_{IJ}(s) = \sigma(s)|t^{(0)}_{IJ}(s)|^2 \tag{6}$$

Resonances are closely related to the saturation of unitarity. That is why we have to unitarize the chiral amplitudes. There are many procedures in the literature to impose Eq.5 which very often lead to different results. Obviously, that is one of the main criticisms to unitarization.

There is, however, a method that has been tested in ChPT and is able to reproduce the $\rho$ and $K^*$ resonances. It is based on dispersion theory and apart from satisfying Eq.5, it also provides the correct unitarity cut on the complex $s$ plane, as well as poles in the second Riemann sheet.

## B The inverse amplitude method

If we consider an amplitude in the complex $s$ plane, the existence of a threshold is reflected as a cut in the real positive axis. The amplitude has two Riemann sheets that are connected through the cut. By crossing symmetry, there is also another cut on the left real axis.

A dispersion relation is nothing but the Cauchy theorem applied in one of the sheets. Thus, the values of that function in any point will be given by the integrals of $\mathrm{Im} t(s)$ over the cuts. Of course, these values are not known exactly, and with our chiral expansion we only get a crude approximation replacing $\mathrm{Im} t(s) \simeq \mathrm{Im} t^{(1)}(s)$

The relevant point is to realize that the inverse amplitude can be calculated *exactly* on the *elastic cut*. Indeed, using Eqs.5 and 6 we find

$$\mathrm{Im}\frac{1}{t_{IJ}} = -\frac{\mathrm{Im} t_{IJ}}{|\, t_{IJ}\,|^2} = -\sigma = -\frac{\mathrm{Im} t^{(1)}_{IJ}}{|\, t^{(0)}_{IJ}\,|^2} \tag{7}$$

Apart from poles, the cut structure of the amplitude $t(s)$ and that of the function $|\, t^{(0)}_{IJ}\,|^2 / t_{IJ}(s)$ are the same.

Their right cut contributions only differ on a sign, and therefore, solving for $t(s)$ one obtains [10, 8]:

$$t_{IJ} \simeq \frac{t_{IJ}^{(0)}}{1 - t_{IJ}^{(1)}/t_{IJ}^{(0)}} \tag{8}$$

Notice that if we expand again at small momenta, we recover the chiral expansion in Eq.3. Therefore, the Inverse Amplitude Method (IAM) displays the correct low energy behavior. We can perform again the very same analysis of the preceeding section. The difference from ChPT appears at higher energies, but now we have several advantages:

- It satisfies the elastic unitarity constraint.
- The elastic right cut has been calculated exactly.
- It can reproduce poles.

Remember that the amplitude is extended continuously to the second Riemann sheet through the cut. Hence, from the second point above, we expect to obtain a very good approximation near the cut in the second Riemann sheet. But resonances are characterized as poles close to the real axis and in the second sheet. That is why this method is able to reproduce resonances.

Of course, the method has several limitations too [8]. First, the left cut is still an approximation. Next, we have neglected possible poles in G, which are indeed present [11]. Fortunately these effects are not dominant at high energies, where the right cut and resonance contributions dominate. They will however introduce some uncertainty in the position and width of the resonances. There are also other rather technical issues that we will not address here [8].

Let us now review how the IAM works. We want to know how well it reproduces the high energy behavior using *only low energy data*, since that could be the situation at LHC. In particular, we are interested on whether we can establish the existence of resonances even though they are not directly seen.

## C The IAM in Chiral Perturbation Theory

When it is applied to pion physics [12, 8], the IAM is able to reproduce a $\rho$ resonance just using low energy data. In Figure 1.a, the results of plain ChPT are plotted as a dotted line. It has been calculated with the parameters proposed in [17], which have been obtained *only* from *low energy data* ($\lesssim$400 GeV). The other two lines are the IAM prediction. The dashed one has been obtained with the same parameters and the continuous one with an slightly different set [18]. As far as the only input in the calculations is low energy data, the existence of the $\rho$ can be seen as a *prediction* of the IAM. The qualitative behavior of the phase shift is obviously correct. Notice that the value of its mass does not lie very far from the actual value. The theoretical error is hard to estimate, but we have found, varying the parameters inside their error bars, that it is never bigger than 20% [8].

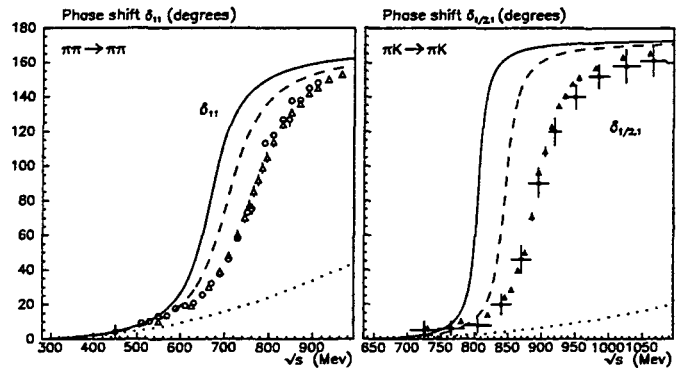


**Figure 1.**-a) $\delta_{11}$ phase shift in $\pi\pi$ scattering. The data comes from: [13] ($\triangle$), [14] ($\circ$); b)$\delta_{1/2,1}$ in $\pi K$ scattering. [15] ($\bullet$),[16] ($\triangle$). The dotted curves are plain ChPT. The others are the IAM with two sets of chiral parameters.

Of course, it is possible to get a better fit (see [8]) but then high energy data should also be used as an input.

The case of $\pi\pi$ scattering is specially relevant since it can be described with the very same $SU(2)$ scheme of symmetry breaking of the EWSBS. However, the IAM also works in other models. In Figure 1.b it is shown how it is also possible to reproduce the $K^*(892)$ resonance in $\pi K$ elastic scattering using $SU(3)$ ChPT [12, 8]. The uncertainties are again of the same order.

It can also be checked [8] that the amplitudes present the appropriate analytical structure including the corresponding poles in the second Riemann sheet.

We have therefore shown that the IAM is not just a simple numerical trick to unitarize amplitudes. It contains all the analytic structure needed to extract the correct high energy behavior from low energy data.

## D Resonances in the strong EWSBS.

Throughout this section we will be using the Equivalence Theorem [19]. It states that the $V_L V_L$ amplitudes are those of GB up to $\mathcal{O}(M_V/\sqrt{s})$. At high energies those terms can be neglected and the $V_L V_L$ amplitudes look exactly as those of $\pi\pi$ scattering in the massless limit.

At first sight it is not evident that such a high energy limit can be used with a low energy approach like chiral lagrangians. However, it has been shown [3, 20] that there is a common applicability window, and that the theorem remains the same when working at lowest order in the electroweak couplings, which is our case.

Let us then apply the IAM to the reference models of Table I. In Figure 2 we can see (solid lines) how the IAM yields an scalar resonance in the Higgs model, and a technirho in the QCD model [21]. There are no other resonances present. We have found again that the IAM yields the correct result. Let us then scan the parameter space to get a qualitative description of the general resonance spectrum of an strong EWSBS.

We will only concentrate on the $(I, J) = (0, 0)$ and $(1, 1)$ channels. The $I = 2$ channel is more subtle and will be

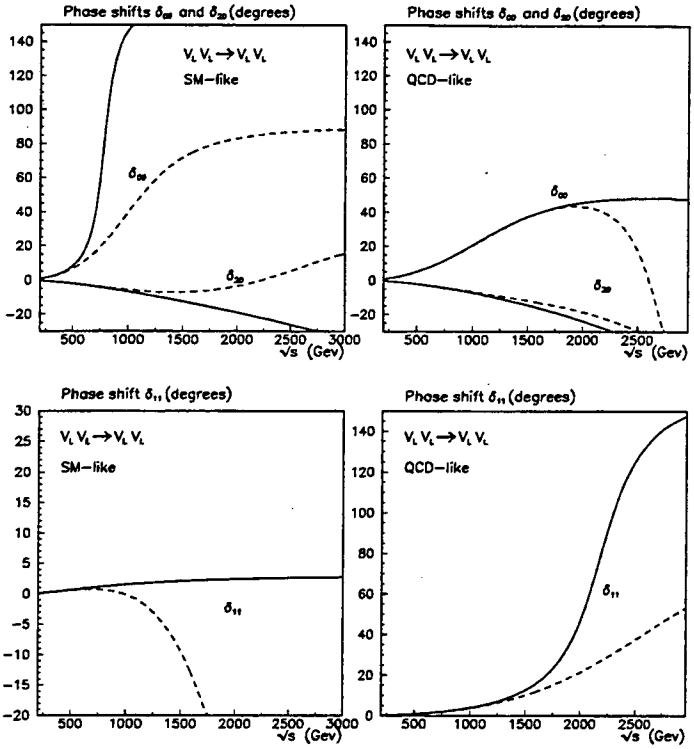


**Figure 2.-** $V_L V_L \to V_L V_L$ phase shifts in the heavy Higgs SM (left) and a QCD-like model(right). Notice their respective scalar and the vector resonances. The dashed lines are the chiral amplitudes and the solid lines are the IAM results.

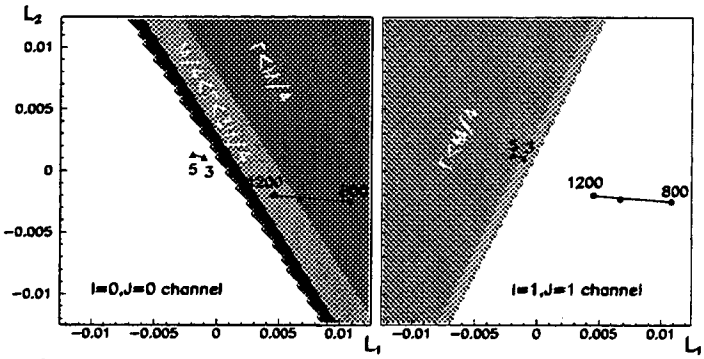


**Figure 3.-** Resonant states in the $L_1, L_2$ plane, both for the $(I, J) = (0, 0)$ and $(1, 1)$ channels. The dark color areas correspond to narrow resonances. Lighter areas are broad resonances and black areas stand for saturation. White is no resonance or saturation below 3TeV

given elsewhere.

In Figure III we have plotted in the $L_1, L_2$ plane the expected unitarity behavior up to 3 TeV of the $VV$ amplitudes. There are several possibilities: No resonance (white), a saturation of unitarity (black), a broad resonance (light) or a narrow resonance (dark). By narrow or broad, we mean that the width is smaller or bigger than 25% of the mass, respectively. We understand by saturation that the unitarity bound is reached, but a resonance there would have a width of 75% its mass or more. We have also shown the position of the SM with $M_H = 800$ to 1200GeV (black dots), as well as QCD-like models with 3 or 5 technicolors (black triangles).

From the graphs it seems that there are many different phenomenological scenarios. Maybe there is just one resonance, two resonances or no resonances at all. It could happen that one channel saturates unitarity while the other has a resonance, etc...

In conclusion, the effective lagrangian approach supplemented with the IAM, emerges as a very powerful and simple tool to explore a great variety of strongly interacting scenarios.

## III ACKNOWLEDGMENTS

I would like to thank the Theory Group at Berkeley for their kind hospitality and the Jaime del Amo Foundation for a fellowship. This work has been partially supported by the Ministerio de Educación y Ciencia (Spain) (CICYT AEN93-0776). Partial support by US DOE under contract DE-AC03-76SF00098 is gratefully acknowledged.

## IV REFERENCES

[1] P.Sikivie et al. *Nucl. Phys.* **B173** (1980) 189.

[2] M.S.Chanowitz, M.Golden and H.Georgi, *Phys.Rev.* **D36** (1987) 1490.

[3] A.Dobado and J.R.Peláez, *Nucl. Phys.* **B425** (1994) 110.

[4] A.Dobado and M.J.Herrero, *Phys. Lett.* **B228** (1989) 495 and **B233** (1989) 505; J.Donoghue and C.Ramirez, *Phys. Lett.* **B234** (1990) 361.

[5] S.Weinberg, *Physica* **96A** (1979) 327; J.Gasser and H.Leutwyler, *Ann. of Phys.* **158** (1984) 142; *Nucl. Phys.* **B250** (1985) 465 and 517.

[6] T.Appelquist and C.Bernard, *Phys. Rev.* **D22** (1980) 200; A.C.Longhitano, *Nucl. Phys.* **B188** (1981) 118.

[7] M.J.Herrero and E.Ruiz Morales, *Nucl.Phys.* **B418** (1994) 431; *Nucl.Phys.* **B437** (1995) 319.

[8] A.Dobado and J.R.Peláez, hep-ph/9604416.

[9] CMS Technical Proposal. CERN/LHC94-38.LHCC/P1. (1994); A.Dobado, M.J.Herrero, J.R.Peláez, E.Ruiz Morales and M.T.Urdiales *Phys. Lett.* **B352** (1995) 400; A.Dobado and M.T.Urdiales hep-ph/9502255 (To appear in *Z.Phys.*)

[10] Tran N. Truong, *Phys. Rev. Lett.* **61** (1988) 2526, ibid **D67** (1991) 2260.

[11] M.Boglione and M.R.Pennington, hep-ph/9607266.

[12] A.Dobado, M.J.Herrero and T.N.Truong, *Phys. Lett.* **B235** (1990) 134; A.Dobado and J.R.Peláez, *Phys. Rev.* **D47** (1992) 4883.

[13] Protopopescu et al., *Phys.Rev.* **D7** (1973) 1279.

[14] P.Estabrooks and A.D.Martin, *Nucl.Phys.* **B79** (1974) 301.

[15] R. Mercer et al., *Nucl. Phys.* **B32** (1971) 381.

[16] P. Estabrooks et al., *Nucl. Phys.* **B133** (1978) 490.

[17] C.Riggenbach, J.F.Donogue, J.Gasser and B.Holstein, *Phys.Rev.* **D43** (1991) 127.

[18] J.Bijnens, G.Colangelo, J.Gasser, *Nucl. Phys.* **B427** (1994) 427.

[19] J.M. Cornwall, D.N. Levin and G. Tiktopoulos, *Phys. Rev.* **D10** (1974) 1145; C.E.Vayonakis, *Lett. Nuovo Cim.* **17** (1976) 383; B.W. Lee, C. Quigg and H. Thacker, *Phys. Rev.* **D16** (1977) 1519; M.S. Chanowitz and M.K. Gaillard, *Nucl. Phys.* **B261** (1985) 379.

[20] H.J. He, Y.P. Kuang and X.Li, *Phys.Lett* **B329** (1994) 278.

[21] A.Dobado, M.J.Herrero, T.N.Truong, *Z. Phys.* **C50** (1990) 129; A.Dobado, M.J.Herrero, J.Terrón, *Z. Phys.* **C50** (1991) 205; ibid 465.

Ernest Orlando Lawrence Berkeley National Laboratory
One Cyclotron Road | Berkeley, California 94720

Prepared for the U.S. Department of Energy under Contract No. DE-AC03-76SF00098